Neuron, Vol. 35, 1115–1126, December 19, 2002, Copyright ©2002 by Cell Press

Interaction of Postsynaptic Receptor Saturation with Presynaptic Mechanisms Produces a Reliable Synapse

Kelly A. Foster, Anatol C. Kreitzer, and Wade G. Regehr[1]
Department of Neurobiology
Harvard Medical School
Boston, Massachusetts 02115

Summary

Synapses that reliably activate their postsynaptic targets typically release neurotransmitter with high probability, are not very sensitive to changes in calcium entry, and depress. We have determined the mechanisms that give rise to these characteristic features at the climbing fiber to Purkinje cell synapse. We find that saturation of presynaptic calcium entry, of presynaptic release, and of postsynaptic receptors combine to produce a postsynaptic response that is near maximal. Postsynaptic receptor saturation also accelerates recovery from depression, in part by accentuating a rapid calcium-dependent recovery phase. Thus, postsynaptic receptor saturation interacts with presynaptic mechanisms to produce highly reliable synapses that can effectively drive their targets even during sustained activation.

Introduction

Presynaptic action potentials trigger neurotransmitter release with a high probability at many synapses. These "high p" synapses share two common properties: repetitive presynaptic activity results in depression (Eccles et al., 1941; Feng, 1941; Zucker and Regehr, 2002) and synaptic efficacy saturates with increasing extracellular calcium (Ca_e) (Dodge and Rahamimoff, 1967; Jenkinson, 1957). Many of these synapses produce large postsynaptic responses that reliably drive their targets to fire even during high-frequency activity (Brenowitz and Trussell, 2001; Eccles et al., 1966a; Taschenberger and von Gersdorff, 2000). For other high p synapses, depression can affect the transmission of information between neurons (Abbott et al., 1997; Chung et al., 2002; Tsodyks and Markram, 1997). Although high p synapses are prominent throughout the nervous system, the mechanisms that underlie their characteristic behavior are poorly understood.

There are several possible explanations for the relative insensitivity of high p synapses to apparent changes in calcium entry. The leading hypothesis is that release of neurotransmitter is limited by the number of release-ready vesicles (Zucker and Regehr, 2002). Another possibility is that calcium entry saturates with increases in extracellular calcium levels (Ca_e), as has been shown at some synapses (Mintz et al., 1995; Schneggenburger et al., 1999). In addition, multivesicular release can lead to postsynaptic receptor saturation (Wadiche and Jahr, 2001), which could limit the EPSC amplitude. The relative contributions of these various mechanisms to saturation of the postsynaptic response are not known.

The second common property of high p synapses, short-term depression, has also been studied extensively (Zucker and Regehr, 2002). Depression is often attributed to the depletion of release-ready vesicles (Betz, 1970; Liley and North, 1953). However, many mechanisms can influence the magnitude of depression, and depletion models are often inadequate (Zucker and Regehr, 2002). This is illustrated by the recent discovery that multivesicular release combined with postsynaptic receptor saturation can reduce the magnitude of depression (Wadiche and Jahr, 2001). Recovery from depression is another important determinant of how synapses function during repetitive activation. Recovery is often exponential with a time constant of several seconds (Betz, 1970; Kusano and Landau, 1975; Zucker and Regehr, 2002), but it can be accelerated in an activity-dependent manner by a build up of presynaptic calcium (Dittman and Regehr, 1998; Stevens and Wesseling, 1998; Wang and Kaczmarek, 1998). The manner in which postsynaptic receptor saturation influences recovery from depression has not been studied.

Here we characterize the mechanisms underlying basic features of synaptic transmission at the climbing fiber to Purkinje cell synapse, which is a high p synapse that is amenable to study. Each Purkinje cell receives a strong input from a single climbing fiber that can be activated in isolation (Eccles et al., 1966a; Ramon y Cajal, 1911). It is also possible to optically measure calcium levels in individual climbing fibers (Kreitzer et al., 2000), making it possible to assess saturation of calcium influx. At this synapse, short-term depression is presynaptic in origin (Dittman and Regehr, 1998; Hashimoto and Kano, 1998; Silver et al., 1998), multivesicular release and postsynaptic receptor saturation occur (Wadiche and Jahr, 2001), and calcium-dependent recovery from depression is present (Dittman and Regehr, 1998).

Our findings indicate that the interaction of multiple mechanisms must be considered in order to understand the characteristic features of this high p synapse. Saturation of calcium entry, presynaptic release and postsynaptic receptors combine to cause this synapse to be relatively insensitive to changes in calcium entry and to elicit a maximal postsynaptic response in standard conditions. Postsynaptic receptor saturation also speeds recovery from depression, in part by accentuating a rapid calcium-dependent component of recovery. Our findings indicate that postsynaptic receptor saturation acts in concert with presynaptic mechanisms to allow high-reliability synapses to drive their targets even during sustained presynaptic activity.

Results

We investigated the calcium dependence of synaptic strength and short-term plasticity at the climbing fiber to Purkinje cell synapse. Single climbing fibers were stimulated, and EPSCs were measured with whole-cell

[1]Correspondence: wade_regehr@hms.harvard.edu

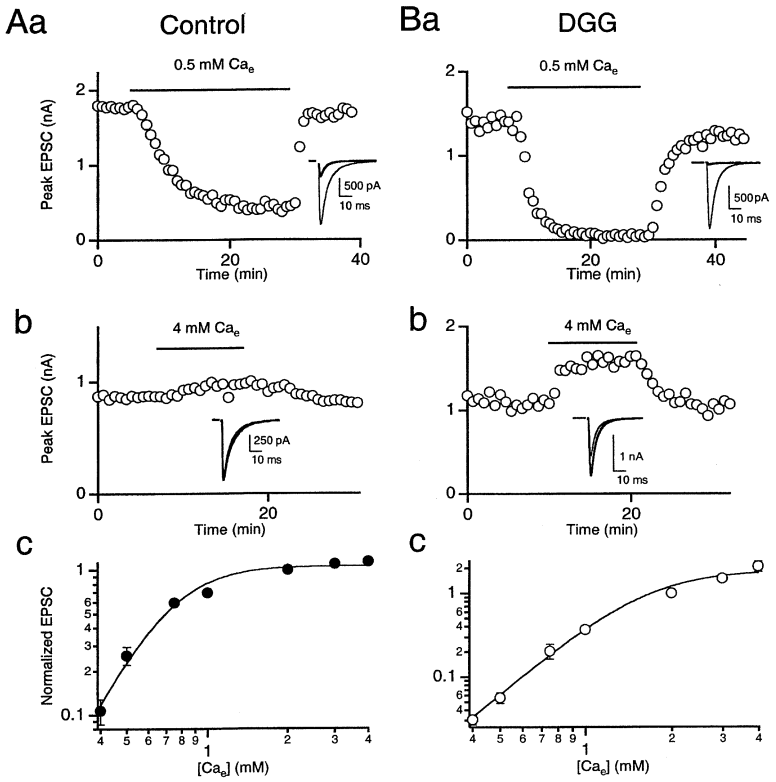

Figure 1. The Effect of Postsynaptic Receptor Saturation on the Relationship between External Calcium and EPSC Amplitude

The effect of Ca_e in control conditions (A) and in the presence of 5 mM DGG to relieve AMPA receptor saturation (B). Representative experiments in (Aa) and (Ba) and in (Ab) and (Bb) show the time course of the EPSC amplitude with the initial conditions being 2 mM Ca_e. Application of 0.5 mM Ca_e (Aa and Ba) and 4 mM Ca_e (Ab and Bb) is denoted by the horizontal line. (Insets) Averaged traces in 2 Ca_e (light trace) and high or low Ca_e (dark trace). The peak EPSC values normalized to those in 2 mM Ca_e are plotted as a function of Ca_e on log scales (Ac and Bc). The data were fit to Equation 2, with $EPSC_{max}$ = 1.1, n = 3.5, and $K_{0.5}$ = 0.72 mM for control conditions and $EPSC_{max}$ = 1.9, n = 2.8, and $K_{0.5}$ = 1.6 mM in the presence of DGG. Each point in (Ac) and (Bc) is the average of three to six experiments. Error bars are SEM. In many cases, error bars are obscured by the symbols.

voltage clamp techniques. Presynaptic calcium transients were monitored with fluo-4 dextran (Kreitzer et al., 2000), which is a low affinity calcium-indicator that provides an accurate measure of the time course of residual calcium signals and allows quantification of changes in calcium entry evoked by an action potential.

Saturation of EPSC Amplitude with Increasing External Calcium

We began by determining the relationship between extracellular calcium levels and EPSC amplitude. At many synapses, the EPSC amplitude is highly sensitive to changes in Ca_e when Ca_e is low and saturates at very high Ca_e. This is also true for the climbing fiber synapse. In representative experiments, decreasing Ca_e from 2 mM to 0.5 mM decreased the peak EPSC to 27% of that in 2 Ca_e, while increasing Ca_e from 2 mM to 4 mM increased the peak EPSC to 108% of that in 2 Ca_e (Figure 1A). The relationship between the peak EPSC and Ca_e, which is summarized in Figure 1Ac, shows that when Ca_e is below 0.75 mM, there is a supralinear relationship between EPSC amplitude and Ca_e, and the EPSC can be approximated by the power law relationship:

$$EPSC = k(Ca_e)^n, \quad (1)$$

where k is a constant and n = 3. A similar relationship was observed by Dodge and Rahamimoff at the neuromuscular junction (Dodge and Rahamimoff, 1967) and subsequently at many other synapses. Another common feature among many synapses is that the EPSC amplitude begins to saturate as Ca_e is increased, and this is also true for the climbing fiber synapse. As a result, Equation 1 does not fit the data over the full range of Ca_e, but the Hill equation:

$$EPSC = EPSC_{max}(Ca_e^n/(Ca_e^n + K_{0.5}^n)), \quad (2)$$

provides a good approximation, with $EPSC_{max}$ = 1.1, n = 3.5, and $K_{0.5}$ = 0.72 mM for control conditions. The $K_{0.5}$ and $EPSC_{max}$ values indicate that in standard conditions (2 mM Ca_e), the EPSC amplitude is near saturation. When Ca_e is below 0.75 mM, the EPSC amplitude is still steeply dependent on extracellular calcium, and this equation reduces to the power law relationship of Equation 1. This behavior indicates that the climbing fiber synapse operates near saturation and has a high baseline probability of release. The underlying mechanism responsible for saturation of climbing fiber synapses and other synapses is not known.

As a first step in examining the underlying mechanism responsible for the saturation of EPSC amplitude, we assessed the contribution of postsynaptic receptor saturation, which has been shown to occur at the climbing fiber synapse (Wadiche and Jahr, 2001). As a result of receptor saturation, the observed EPSC amplitude is not linearly related to the amount of glutamate released from the presynaptic terminal when the probability of release is high and multivesicular release occurs. We took advantage of the speed of low-affinity receptor antagonists (Clements et al., 1992; Diamond and Jahr, 1997). We used DGG, which is a low-affinity AMPA receptor antagonist with rapid kinetics (Liu et al., 1999; Watkins et al., 1990) that can relieve receptor saturation (Wadiche and Jahr, 2001). By competing with glutamate, DGG makes the relationship between the amount of glutamate released and the EPSC more linear. In contrast, high-affinity antagonists, such as NBQX and CNQX,

dissociate from receptors more slowly and do not relieve saturation or influence paired-pulse plasticity at the climbing fiber synapse. Saturation also influences the paired-pulse ratio (PPR), defined as the amplitude of the second EPSC divided by the amplitude of the first EPSC, because the first and larger EPSC is more attenuated than the second depressed EPSC. We took advantage of this to determine the concentration of DGG needed to eliminate saturation. We found that the effect of DGG on PPR in 4 Ca_e was maximal at 5 mM DGG (see Experimental Procedures). Based on these studies, we used 5 mM DGG to prevent AMPA receptor saturation, which reduced the EPSC ~5-fold).

We then refined our examination of the relationship between EPSC amplitude and Ca_e, but this time using DGG (5 mM) to prevent AMPA receptor saturation. If AMPA receptor saturation contributes to the relationship between calcium influx and release, the same alteration of Ca_e should produce a larger change of EPSC amplitude in DGG relative to control. As shown in Figure 1B, this was the case. Decreasing Ca_e from 2 mM to 0.5 mM decreased the peak EPSC to 4% of that in 2 Ca_e (Figure 1Ba), while increasing Ca_e from 2 mM to 4 mM increased the peak EPSC to 150% of that in 2 Ca_e (Figure 1Bb). The extent of EPSC saturation with increasing Ca_e was less pronounced in the presence of DGG (Figure 1Bc) than in control conditions (Figure 1Ac). In the presence of DGG, Equation 2 is well fit by $EPSC_{max} = 1.9$, $n = 2.8$, and $K_{0.5} = 1.6$ mM. The increase of $K_{0.5}$ from 0.72 to 1.6 in DGG indicates that in control conditions AMPA receptor saturation makes a substantial contribution to EPSC saturation.

Saturation of Calcium Influx

Mechanisms other than AMPA receptor saturation must be responsible for the EPSC saturation that persists in the presence of DGG. One possibility is that calcium influx is not linearly related to Ca_e, as observed previously at other synapses (Mintz et al., 1995; Schneggenburger et al., 1999). We therefore used fluo-4 dextran, an indicator with a 3 μM dissociation constant that provides a linear measure of calcium entry (Kreitzer et al., 2000), to determine how Ca_{influx} varies with Ca_e at the climbing fiber synapse. Representative experiments show that lowering Ca_e from 2 mM to 0.5 mM decreased Ca_{influx} to 31% of that observed in 2 Ca_e (Figure 2A), and raising Ca_e from 2 mM to 4 mM increased Ca_{influx} to 162% (Figure 2B). A summary of the Ca_e dependence of Ca_{influx} (Figure 2C) reveals a sublinear relationship, which indicates that Ca_{influx} through voltage-gated calcium channels begins to saturate as Ca_e is increased. The data were fit to a Michaelis-Menten equation of the form $Ca_{influx} = A/(1 + K_d/Ca_e)$ with a K_d of 2.0 mM Ca_e. Thus, saturation of calcium entry also contributes to the sublinear relationship between EPSC amplitude and Ca_e at high Ca_e.

Contributions of Different Mechanisms to EPSC Saturation

We have now examined the effect of varying Ca_e on calcium influx and on the EPSC in both control conditions and when AMPA receptor saturation is eliminated. This information can be used to determine the contributions of presynaptic and postsynaptic mechanisms to the overall saturation of the EPSC.

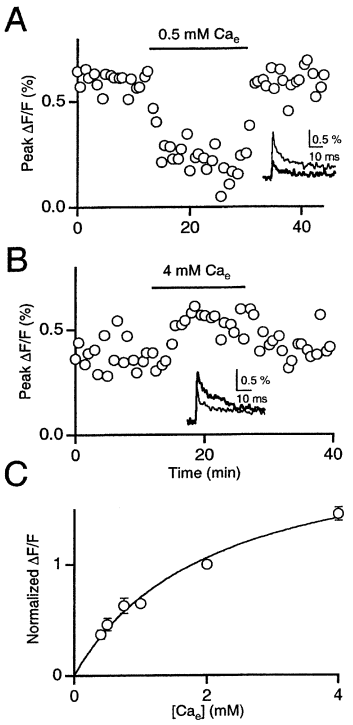

Figure 2. The Relationship between External Calcium and Presynaptic Calcium Influx

(A and B) Time course of peak ΔF/F evoked by single stimuli measured with fluo-4 dextran from individual climbing fibers. Initial conditions were 2 mM Ca_e, and the horizontal line denotes the time during which 0.5 mM Ca_e (A) and 4 mM Ca_e (B) were applied. (Insets) Average traces in 2 Ca_e (light trace) and 4 or 0.5 Ca_e conditions (dark traces).

(C) The peak ΔF/F values normalized to those in 2 mM Ca_e are plotted as a function of Ca_e. The data were fit to the equation $Ca_{influx} = A_{max}/(1 + K_d/Ca_e)$ with $A_{max} = 2.1$ and $K_d = 2.0$ mM.

Plotting EPSC amplitude as a function of Ca_{influx} allowed us to assess the contribution of mechanisms other than saturation of calcium influx to saturation of the EPSC amplitude (Figure 3). As a result of saturation of calcium entry, the EPSC amplitude is more steeply dependent on Ca_{influx} than on Ca_e, both in control conditions (Figure 3A) and in the presence of DGG (Figure 3B).

We next compared EPSC saturation in control conditions and when AMPA receptor saturation was eliminated. This was done by scaling the EPSCs measured in DGG to those measured in control conditions for the lowest two values of calcium influx, where AMPA receptor saturation is minimal (Figure 3C). The plot of EPSC amplitude measured in control conditions (Figure 3C, closed circles) shows significantly more saturation than that measured in DGG (Figure 3C, open circles). For both experimental conditions, the data were well fit by the Hill equation of the form

$$EPSC = EPSC_{max} \times Ca_{influx}^{n}/(Ca_{influx}^{n} + K_{0.5}^{n}). \quad (3)$$

In control conditions, $EPSC_{max} = 1.1$, $n = 4.5$, and $K_{0.5} = 0.6$, which corresponds to an EPSC that is half maximal

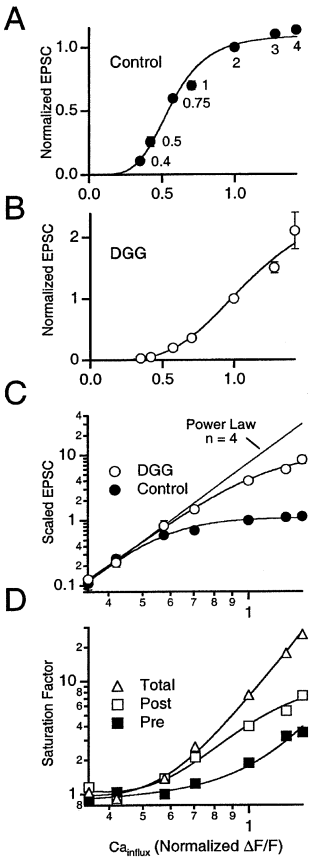

Figure 3. Multiple Mechanisms Contribute to EPSC Saturation

The peak EPSCs are plotted as a function of Ca_{influx} for control conditions (A) and in the presence of 5 mM DGG to relieve AMPA receptor saturation (B). The numbers next to the symbols in (A) indicate the corresponding concentration of Ca_e. The data were fit to Equation 3. For control conditions, $EPSC_{max} = 1.1$, $n = 4.5$, and $K_{0.5} = 0.6$, and in the presence of DGG, $EPSC_{max} = 2.6$, $n = 3.8$, and $K_{0.5} = 1.1$. (C) EPSC amplitudes in control conditions (closed circles) and in the presence of 5 mM DGG (open circles) are plotted as a function of Ca_{influx} on a log scale, with fits as in (A) and (B). The DGG curve is normalized such that the values in 0.4 and 0.5 Ca_e overlap with those of the control curve. The straight line represents the fit of the first three points of the DGG curve to a power law function where $n = 4$. (D) The ratio of the power law fit of (C) and the control curve provides a measure of the total saturation factor arising from all mechanisms (triangles). The contribution of postsynaptic receptor saturation to the EPSC amplitude was computed by calculating the ratio of the EPSC amplitudes measured in DGG to those measured in control conditions (open squares). The contribution of presynaptic receptor saturation was computed by calculating the ratio of the power law fit and EPSC amplitudes measured in DGG (solid squares). Curves are the ratio of the appropriate curves in (C).

at Ca_e of 0.75 mM. In DGG, $EPSC_{max} = 2.6$, $n = 3.8$, and $K_{0.5} = 2.6$, which corresponds to an EPSC that is half maximum at Ca_e of more than 3 mM. Both in control conditions and in the presence of DGG, when Ca_e is below 0.75 mM, there is a supralinear relationship between EPSC amplitude and Ca_e, and the EPSC can be approximated by the power law relationship where $n = 4$ (Figure 3C, straight line). This line represents the EPSC amplitude that we would expect if no mechanism limited the amplitude of the EPSC.

We used the curves in Figure 3C to estimate the total saturation (after taking into account saturation of calcium entry) and the contributions of pre- and postsynaptic factors to this saturation. The ratio of the power law curve to the EPSC amplitudes measured in control conditions provides a measure of the total saturation (Figure 3D, triangles). The contribution of AMPA receptor saturation was estimated from the ratio of the EPSC amplitudes in DGG and in control conditions (Figure 3D, open squares). Similarly, the ratio of the power law fit to the EPSC amplitudes in DGG (Figure 3D, closed squares) provides a measure of additional factors that limit the EPSC amplitude. These factors likely reflect presynaptic mechanisms (see Discussion). In this manner, we estimate that in standard conditions (2 Ca_e) presynaptic ($\sim$2-fold) and postsynaptic ($\sim$4-fold) mechanisms lead to an EPSC that is smaller than that predicted by the power law by a factor of 7.

The Influence of AMPA Receptor Saturation and External Calcium on Paired-Pulse Plasticity

The second characteristic of high p synapses we studied was paired-pulse plasticity. Previous studies have shown that paired-pulse plasticity can be influenced by changing Ca_e and by AMPA receptor saturation (Wadiche and Jahr, 2001; Zucker and Regehr, 2002). We therefore investigated the effect of DGG and varying Ca_e on short-term plasticity.

Paired-pulse plasticity was examined by stimulating climbing fibers with pairs of pulses separated by 10 ms. The paired-pulse ratio (PPR) provided a measure of this plasticity. As shown in the representative experiment in Figure 4Aa, in standard conditions (2 Ca_e), the second EPSC (squares) was less than half as large as the first EPSC (circles), and PPR was 0.4 (diamonds). Raising release probability by changing Ca_e from 2 mM to 4 mM decreased PPR to 0.25 (Figure 4Aa, diamonds). A comparison of the traces recorded in 2 mM Ca_e (fine trace) and 4 mM Ca_e (bold trace) shows that there was a slight increase in the amplitude of the first EPSC and a slight decrease in the amplitude of the second EPSC (Figure 4A, upper right). The more pronounced depression in 4 mM Ca_e was apparent when the traces were normalized to the peak of the first EPSC (Figure 4A, lower right). When Ca_e was lowered to 0.5 mM, the climbing fiber synapse facilitated (Figure 4Ab) (Hashimoto and Kano, 1998), and PPR increased to $\sim$1.25. Figure 4Ac shows that while the size of the first EPSC increases as Ca_e increases (Figure 4Ac, closed circles), the size of the second EPSC (Figure 4Ac, closed squares) only increases until 0.75 Ca_e. Thus, PPR decreases with increasing external calcium (Figure 4C, closed diamonds).

Paired-pulse plasticity is different in the presence of DGG (Figure 4B) from control conditions (Figure 4A). As shown in the representative experiment (Figure 4Ba), PPR in 2 mM Ca_e is decreased in the presence of DGG to 0.25 (open diamonds) as compared to 0.4 in control conditions. Raising release probability by changing Ca_e from 2 mM to 4 mM decreased PPR to 0.11 (Figure 4Ba, diamonds). PPR in the presence of DGG was 1.5 when Ca_e was lowered to 0.5 mM Ca_e (Figure 4Bb, open diamonds), which was not significantly different from control conditions. In the presence of DGG the amplitude

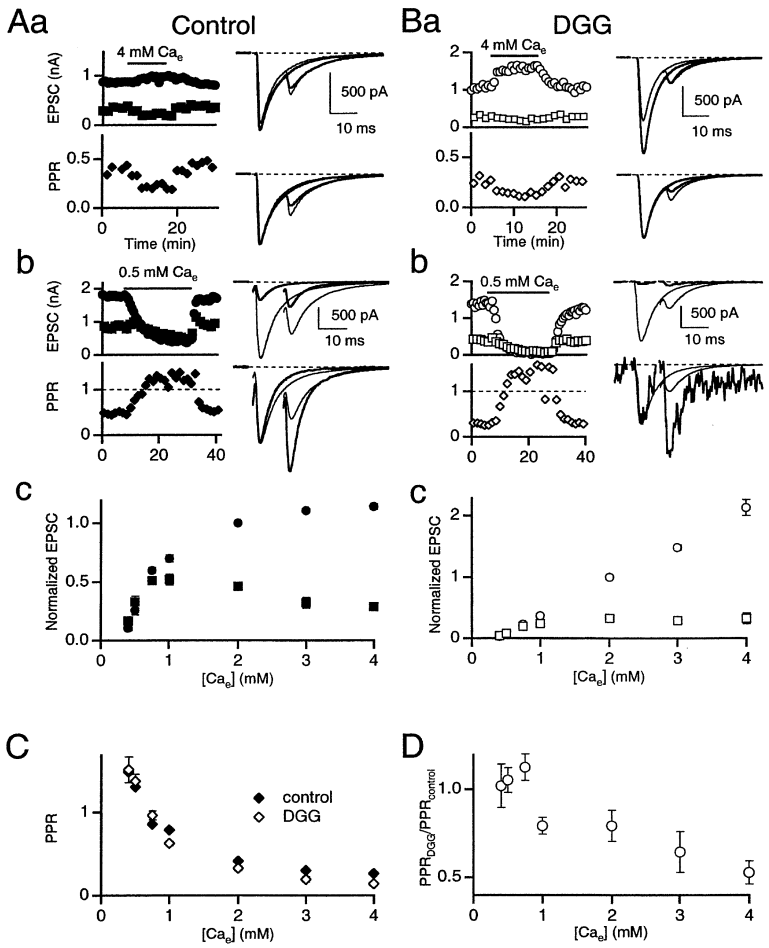

Figure 4. The Effect of Postsynaptic Receptor Saturation on Paired-Pulse Plasticity

The effect of external calcium in control conditions (A) and in the presence of 5 mM DGG to relieve AMPA receptor saturation (B). Representative experiments in (Aa) and (Ba) and in (Ab) and (Bb) show the effect of Ca_e on the amplitudes of a pair of EPSCs separated by 10 ms. (Top left) Time course of the peak of the first EPSC (circles) and the second EPSC (squares). The initial conditions are 2 mM Ca_e, and application of 4 mM Ca_e (Aa and Ba) and 0.5 mM Ca_e (Ab and Bb) is denoted by the horizontal line. (Bottom left) The time course of the paired-pulse ratio (PPR, $EPSC_2/EPSC_1$, diamonds). (Top right) Average traces before (light trace) and during (bold trace) application of 4 or 0.5 Ca_e. (Bottom right) Same traces replotted such that the peak of the first EPSC in 4 or 0.5 Ca_e is normalized to the peak of the first EPSC in 2 Ca_e. (Ac and Bc) Summary of the amplitude of the first EPSC (circles) and the second EPSC (squares) in different Ca_e. Amplitudes are normalized to the size of the first EPSC in 2 mM Ca_e. (C) PPR is plotted as a function of Ca_e in control conditions (closed diamonds) and in the presence of 5 mM DGG (open diamonds). (D) The ratio of the PPR in DGG to the PPR in control conditions ($PPR_{DGG}/PPR_{control}$) is plotted as a function of Ca_e. Each point in (C) and (D) is the average of two to five experiments. Most error bars are obscured by the symbols.

of the first pulse continues to increase while the amplitude of the second plateaus at 0.75 Ca_e (Figure 4Bc). Thus, as in control conditions, PPR decreases as Ca_e increases in the presence of DGG (Figure 4C). However, there are differences in the amplitude of PPR in the two conditions. These differences are most easily observed by plotting the ratio of PPR in DGG to PPR in control conditions ($PPR_{DGG}/PPR_{control}$) as a function of Ca_e (Figure 4D). In low Ca_e, the PPR in the two conditions is very similar, reflecting the lack of saturation when the probability of release is low. However, as release probability is increased, $PPR_{DGG}/PPR_{control}$ drops to about 0.5.

This is consistent with postsynaptic receptor saturation making no significant contribution to short-term plasticity when the initial probability of release is low but becoming important when the release probability is high (Wadiche and Jahr, 2001). In addition to revealing the effects of saturation on paired-pulse plasticity, these data serve as an additional control for the effects of DGG on transmission. If DGG were affecting presynaptic release, we would expect to see a change in PPR under conditions of low release probability, even though saturation does not play a role under these conditions. No such change is observed. Moreover, even for experimental conditions for which DGG alters paired-pulse plasticity (2 Ca_e), we found in separate control experiments that DGG did not significantly alter presynaptic calcium entry into climbing fibers (95.8% ± 4.6% control, n = 4).

AMPA Receptor Saturation Affects Recovery from Depression

The time course of recovery from depression can have a significant effect on the ability of a synapse to drive firing in its postsynaptic target during repetitive synaptic activation. Although DGG has been shown to affect PPR at short interpulse intervals, the effect of AMPA receptor saturation on recovery from depression has not been assessed. We therefore determined the time dependence of PPR in control conditions and in DGG by delivering pairs of pulses to the climbing fiber at interstimulus intervals ranging from 10 ms to 10 s. As a control, we examined PPR in 0.4 mM Ca_e where postsynaptic receptor saturation is not prominent and found that DGG did not significantly alter the amplitude or the time course of PPR (Figure 5A).

In contrast, postsynaptic receptor saturation has a significant impact on recovery from depression (Figure 5B). In 4 mM Ca_e, recovery from depression occurs in two phases and can be approximated with a double exponential (Figure 5B, closed circles). The fast component has a time constant of 89 ms and accounts for 43% of the recovery, and the slow component has a time constant of 2.7 s and accounts for 57%. In DGG,

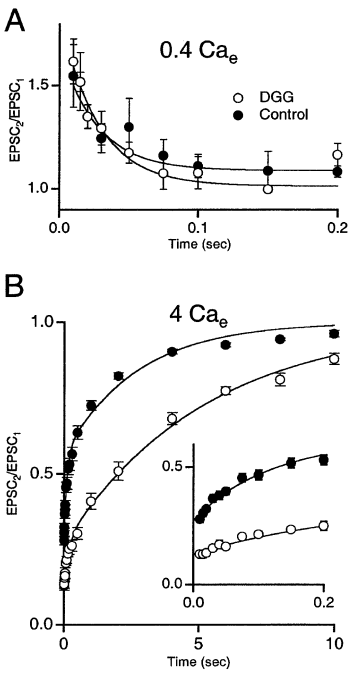

Figure 5. The Time Course of Short-Term Plasticity in Control Conditions and after Relief of Postsynaptic Receptor Saturation

The time course of PPR (PPR = $EPSC_2/EPSC_1$) in 0.4 Ca_e (A) and 4 Ca_e (B) is shown for control conditions (closed circles) and in the presence of 5 mM DGG (open circles). The fits shown in (A) are to the equation $PPR = A_1 + A_2e^{-1/\tau}$, with fit parameters [$A_1$, A_2, τ (ms)] of [1.1, 0.64, 38] in control conditions (n = 6), and [1.1, 1.04, 16] in DGG (n = 6). In (B), the data were fit to the equation $PPR = 1 + A_1e^{-1/\tau1} + A_2e^{-1/\tau2}$. Fit parameters [$A_1$, τ_1(ms), A_2, τ_2(s)] were [−0.33, 89, −0.43, 2.7] for control conditions (n = 17) and [−0.14, 184, −0.73, 5.3] in the presence of DGG (n = 8). (Inset) Shows these same traces on an expanded timescale.

recovery from depression also occurs in two phases, although the fast phase is less prominent (Figure 5B, open circles). The fast component has a time constant of 184 ms and accounts for 16% of the recovery, and the slow component has a time constant of 5.3 s and accounts for 84%. These findings suggest that two mechanisms are involved in recovery from depression, both in control conditions and in the absence of saturation, but that AMPA receptor saturation effectively accelerates the time course of both phases and accentuates the rapid phase (see Discussion).

Dependence of Paired-Pulse Plasticity on Presynaptic Calcium Dynamics

Presynaptic calcium is another important factor that influences both facilitation and recovery from depression. We therefore measured and manipulated presynaptic calcium levels to study the role of calcium in these forms of plasticity.

We first tested the possibility that facilitation and rapid recovery from depression arise from a change in Ca_{influx} into the climbing fiber. We monitored Ca_{influx} for two pulses separated by 20 ms in conditions in which rapid recovery from depression is prominent (2 mM Ca_e) and conditions in which facilitation is prominent (0.4 mM Ca_e). Figure 6A shows an example of such an experiment. Decreasing Ca_e from 2 mM to 0.4 mM reduced Ca_{influx} during both the first pulse (closed circles) and the second pulse (open circles) to ~40% of control. The traces to the right show that the incremental increase in the $\Delta F/F$ was the same for both pulses in the high and low calcium concentrations. The ratio of Ca_{influx} for the two pulses remained close to 1 during the wash-in and wash-out of low calcium (open squares). Therefore, changes in calcium entry for the second of two closely spaced pulses do not contribute significantly to facilitation or rapid recovery from depression.

We next tested the role of elevations of presynaptic calcium levels in short-term plasticity at the climbing fiber synapse. Increases in presynaptic calcium levels have been shown to play a role in short-term plasticity, such as rapid recovery from depression (Dittman and Regehr, 1998; Stevens and Wesseling, 1998; Wang and Kaczmarek, 1998) and facilitation (Katz and Miledi, 1968). Immediately following an action potential, peak local calcium (Ca_{local}) near the release site reaches levels of ~10 μM and decays in a few milliseconds (Fogelson and Zucker, 1985; Heidelberger et al., 1994; Matthews, 1996; Roberts et al., 1990; Simon and Llinas, 1985). Calcium equilibrates throughout the nerve terminal and this residual calcium (Ca_{res}), which is typically several hundred nanomolar, decays to baseline levels over tens of milliseconds (Neher and Augustine, 1992; Tank et al., 1995). EGTA is a slow calcium chelator that speeds the decay of Ca_{res} in the parallel fiber and other synapses (Atluri and Regehr, 1996). Due to its relatively slow calcium binding kinetics (Naraghi, 1997; Smith et al., 1984), EGTA has less of an effect on Ca_{local} (Adler et al., 1991), which drives transmitter release (although effects on EPSC amplitude have been observed at some synapses [Borst and Sakmann, 1996; Chen and Regehr, 1999]). EGTA also attenuates the amplitude of the fast component of recovery from depression at the climbing fiber synapse while having little effect on transmission in 4 mM Ca_e (Dittman and Regehr, 1998), suggesting a role for Ca_{res} in rapid recovery from depression.

Before using EGTA to examine short-term plasticity, we determined the effect of EGTA on Ca_{res} transients in the climbing fiber in 4 Ca_e and on the amplitude of the initial EPSC. As shown in a representative experiment (Figure 6B, left), when 100 μM of the membrane-permeant form of EGTA (EGTA-AM) was bath applied for 10 min, the average half-decay time of the $\Delta F/F$ signal was decreased from 41 ms to 7 ms (Figure 6B, open circles), and the peak $\Delta F/F$ was reduced from 1.1% to 0.7% (Figure 6B, closed circles). The average $\Delta F/F$ transients before and after the application of EGTA-AM (Figure 6B, right; n = 5 experiments) showed a similar reduction in the half-decay time (60 ms to 10 ms) and the amplitude, which was reduced by 33% ± 3%. Reductions in the initial EPSC were sufficiently small (~15% in 4 Ca_e, ~20% in 4 Ca_e + DGG, and ~40% in 0.4 Ca_e) that they were unlikely to contribute significantly to changes in paired-pulse plasticity. These findings show that the primary effect of EGTA is to accelerate the time course of the Ca_{res} and suggest that it can be used to test the role of Ca_{res} in short-term plasticity.

We next tested the effect of EGTA on synaptic plasticity. EGTA eliminated facilitation in 0.4 Ca_e (Figure 6C),

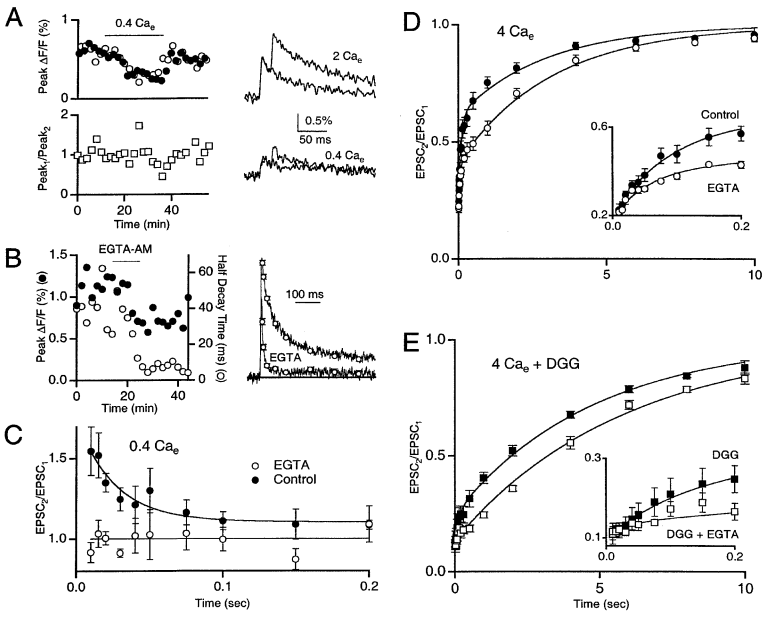

Figure 6. The Dependence of Short-Term Plasticity on Residual Presynaptic Calcium

In (A) and (B), fluo-4 dextran was used to measure calcium transients from individual climbing fibers. (A) (Top left) Time course of incremental ΔF/F increase evoked by the first (closed circles) or second (open circles) of two stimuli separated by 20 ms. The ratio of the change in ΔF/F is indicated below (open squares). The horizontal bar denotes the time during which 0.4 Ca_e was applied. Starting conditions were 2 Ca_e. (Right) Average traces in the indicated conditions. (B) (Left) Time course of the peak (closed circles) and the half-decay time (open circles) of the ΔF/F transient following 100 μM EGTA-AM application in 4 Ca_e. (Right) Average traces from five experiments in control conditions and after application of 100 μM EGTA-AM. Error bars are SEM at the points indicated. (C–E) Time course of PPR before (closed circles) and after (open circles) application of 100 μM EGTA-AM in 0.4 Ca_e (C), 4 Ca_e (D), and 4 Ca_e + 5 mM DGG (E). In (C), the data in control conditions (n = 6) were fit to PPR = $A_1 + A_2e^{-1/\tau}$, with fit parameters [A_1, A_2, τ (ms)] of [1.1, 0.64, 26] and a line with $EPSC_2/EPSC_1 = 1$ approximates the data after exposure to EGTA-AM (n = 5). In (D) and (E), data were fit to PPR = $1 + A_1e^{-1/\tau1} + A_2e^{-1/\tau2}$, with fit parameters [$A_1$, τ_1(ms), A_2, τ_2(s)]. (D) In 4 Ca_e, fit parameters were [−0.42, 87, −0.39, 3.0] for control (n = 5) and [−0.22, 55, −0.59, 3.2] for EGTA (n = 5). (E) In 4 Ca_e + 5 DGG, fit parameters were [−0.15, 116, −0.75, 4.9] for control conditions (n = 4) and [−0.04, 27, −0.86, 5.9] for EGTA (n = 4). Insets in (D) and (E) show the first 200 ms on an expanded timescale.

suggesting that facilitation at the climbing fiber synapse in low Ca_e is the result of enhanced transmitter release driven by elevations in Ca_{res} as has been shown at the parallel fiber synapse (Atluri and Regehr, 1996). In 4 Ca_e, EGTA reduced the amplitude of the fast component from 42% to 27% and reduced the time constant from 89 ms to 55 ms (Figure 6D, open circles); the time course of the slow component of recovery from depression was not greatly affected by EGTA (2.7 s, control; 3.2 s, EGTA). These findings suggest that, at climbing fiber synapses, Ca_{res} drives two distinct forms of synaptic plasticity, facilitation and calcium-dependent recovery from depression (CDR), that are prominent under different experimental conditions.

Although the relative amplitude and time course of the fast component of recovery are changed in the presence of DGG, it is likely that this fast phase of recovery still corresponds to the calcium-dependent process. In order to test this, we examined the effects of EGTA on the recovery curve in the presence of DGG. Under these conditions, the rapid component of recovery is reduced but is still sensitive to EGTA. In the presence of DGG and EGTA, the fast component accounts for only 4% of recovery and decays with a time constant of 27 ms. The slow phase accounts for the remainder of recovery and has a time course similar to recovery in the presence of DGG alone (4.9 s in DGG; 5.9 s DGG + EGTA).

The Effect of Postsynaptic Receptor Saturation during Trains

The effects of DGG on paired-pulse plasticity suggested that postsynaptic receptor saturation might also be important during stimulus trains. We therefore explored the influence of receptor saturation on transmission during and following a 20 Hz train at both 24°C (Figure 7A) and 35°C (Figure 7B), with the results being remarkably similar at these two temperatures. The normalized EPSC

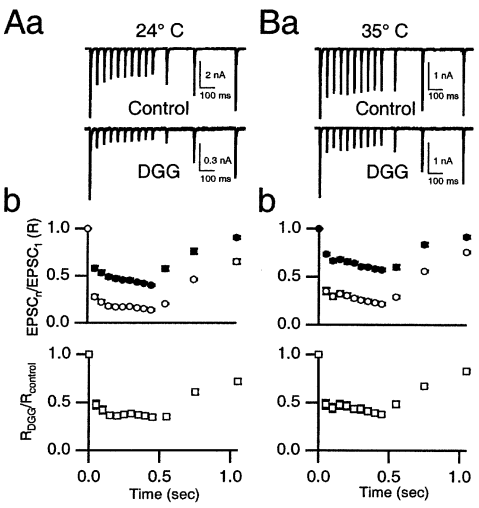

Figure 7. The Effect of Postsynaptic Receptor Saturation during Sustained Activity

Trains of ten pulses at 20 Hz were delivered to the climbing fiber at 24°C (A) and at 35°C (B). (Aa and Ba) The resulting EPSCs are shown for control conditions (top) and in the presence of 5 mM DGG (bottom). Ca_e is 2 mM. In successive trials, test pulses were delivered at either 100, 300, or 600 ms. (Ab and Bb) Paired-pulse ratio (R, $EPSC_n/EPSC_1$) in control conditions (closed circles) and in the presence of 5 mM DGG (open circles) is plotted as a function of time (top, n = 4). The ratio of the magnitudes of depression in DGG to those in control ($R_{DGG}/R_{control}$) is plotted as a function of time (open squares, bottom). Error bars are SEM. In many cases, error bars are obscured by the symbols.

amplitude ($R = EPSC_n/EPSC_1$) in DGG (R_{DGG}) was much smaller than in control conditions ($R_{control}$). The effects of saturation become slightly larger later in the train. This is most evident when the ratio of the normalized EPSC amplitudes in the two conditions ($R_{DGG}/R_{control}$) is plotted as a function of time. The effect of saturation on transmission is also evident following the train. These results suggest that under control conditions, saturation contributes to the reliability of the EPSC and minimizes the considerable attenuation of the EPSC that would occur during repetitive activation if saturation were absent.

Physiological Significance

We next examined the role of saturation and recovery from depression in maintaining the response of a Purkinje cell to climbing fiber activation under physiological conditions. Climbing fibers in vivo typically fire at relatively low frequencies (1 Hz) with periodic short bursts of several spikes at rates as high as 15 Hz (Armstrong and Rawson, 1979; Schwarz and Welsh, 2001). Climbing fiber activation depolarizes its Purkinje cell target and evokes a characteristic response known as a complex spike, which is typically followed by a period of inactivity (Granit and Phillips, 1956; Ito, 1984). The climbing fiber is such a powerful synapse that it is not obvious that the changes in synaptic strength arising from saturation and recovery from depression would affect the manner in which a climbing fiber activates a Purkinje cell. We therefore examined the effects of a physiological pattern of activity on climbing fiber EPSCs in control conditions and when saturation was eliminated and then determined if such reductions in synaptic strength altered climbing fiber efficacy measured in current clamp recordings.

We began by examining the EPSCs evoked by a physiological activity pattern (3 pulses at 15 Hz followed by a test pulse at 100 ms) at 35°C in control conditions and when saturation was eliminated by DGG (Figure 8A). In control conditions, the test pulse was 78% ± 1.8% of the initial pulse in the train, whereas in DGG the test pulse was 47% ± 1.3% of the initial response. Our strategy was to mimic these effects using appropriate concentrations of the AMPA receptor antagonist NBQX, which we determined as in Figure 8B.

We then determined if the reductions of synaptic strength for the fourth pulse of the train in control conditions and in DGG (Figure 8A) had any effect on the climbing fiber response. We mimicked the depression in control conditions and DGG by using, respectively, 50 nM NBQX (reduced to ~78% control) and 250 nM NBQX (reduced to ~47% control). Purkinje cells were spontaneously active at 10 to 40 Hz. As shown for the example of Figure 8C, in control conditions climbing fiber activation (arrow head) prevented the Purkinje cell from firing for 480 ms, as measured from the time of the stimulus until the time of the next spontaneous spike (left). The complex spike arising immediately after climbing fiber activation is shown on an expanded trace (right). Application of 50 nM NBQX caused little change in the complex spike waveform (8C, right), and the duration of the quiet period following climbing fiber activation was similar to control conditions. In 250 nM NBQX, however, climbing fiber activation no longer elicited a com-

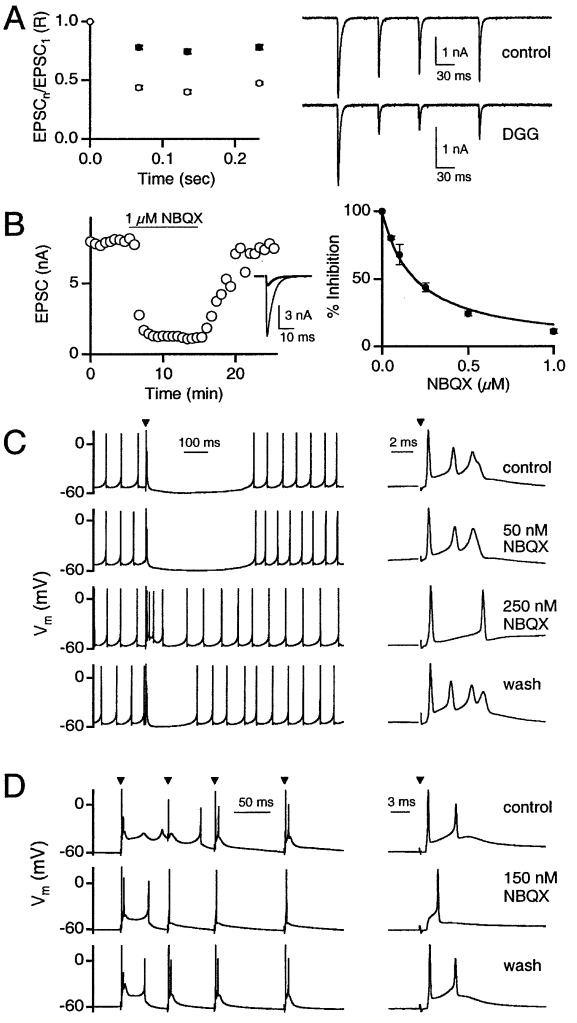

Figure 8. The Contribution of Saturation to the Complex Spike during Trains of Realistic Activity

Experiments were performed in 2 mM Ca_o at 35°C. (A) (Left) EPSCs elicited by trains of three pulses at 15 Hz followed by a test pulse 100 ms later are shown in control conditions (closed circles) and in the presence of 5 mM DGG (open circles). Each point is the average of four experiments, and error bars are the SEM. (Right) Representative EPSCs in control and DGG. (B) (Left) Representative experiment showing the time course of the EPSC amplitude. Application of 1 μM NBQX is denoted by the horizontal line. (Insets) Averaged traces in control conditions (light trace) and in the presence of 1 μM NBQX (dark trace). (Right) The data are plotted as a function of NBQX concentration and fit to the equation $EPSC = 100/(1 + NBQX/K_d)$, where $K_d = 0.2$ μM. Each point is the average of three experiments. Error bars are SEM. (C) The effect of the complex spike on spontaneous Purkinje cell firing in control conditions, 50 nM NBQX, 250 nM NBQX, and after washout of NBQX. Small currents (less than 40 pA) were used to maintain the firing rate at a constant level. Arrowheads indicate the time at which the stimulus was applied. (Right) Traces on an expanded timescale to show the complex spike. (D) Trains of climbing fiber stimuli consisting of three pulses at 15 Hz followed by a stimulus 100 ms later in control conditions (top), in the presence of 150 nM NBQX (middle) and following washout of NBQX (bottom). (Right) Traces on an expanded timescale to show the complex spike in response to the fourth stimulus. Stimulus artifacts have been blanked for clarity.

plex spike but rather evoked a series of simple spikes (8C, right). Similarly, the climbing fiber response caused very little change in the subsequent activity of the cell. This effect was partially reversed upon washout. In four such experiments, we found that the complex spike and the duration of the quiescent period varied significantly between cells in control conditions (1.1 ± 0.5 s). Nonetheless, in all cells, 250 nM NBQX was sufficient to affect the complex spike and subsequent silent period (29% ± 2% of control), whereas 50 nM NBQX did not significantly alter the duration of the silent period (90% ± 14% of control). These results suggest that in the absence of AMPA receptor saturation the depression arising from such a brief train would be large enough to prevent the climbing fiber from reliably eliciting a complex spike and would diminish the influence of the climbing fiber on subsequent Purkinje cell activity.

Although we have shown that 50% reductions in synaptic strength can reduce the efficacy of climbing fiber activation, we also wanted to examine the climbing fiber response evoked by brief trains. We therefore measured in current clamp the response of Purkinje cells to climbing fiber activation with the activity pattern of Figure 8A. In these experiments, a small holding current was used to maintain the Purkinje cells at −60mV to eliminate spontaneous activity. The response to such a train is shown in Figure 8D, upper left. Each of the stimuli evoked a strong response in the Purkinje cell, and the response to the fourth stimulus is shown on an expanded timescale to the right. We next wanted to assess the effect of eliminating saturation on the Purkinje cell response. As noted above, the fourth EPSC is 78% of the first in control conditions and 47% of the first in DGG. In this experiment, the AMPA conductance during the fourth pulse in current clamp is already reduced to 78% by the preceding train. In order to mimic the effects of eliminating saturation on the fourth pulse, we needed to further reduce the AMPA receptor conductance during this pulse to 60% of its control value (47%/78%). We used 150 nM NBQX to mimic this reduction (Figure 8D, middle). Although all of the spikes in the train are affected by NBQX, we focus on the fourth climbing fiber response. In 150 nM NBQX, climbing fiber activation produced only a single delayed spike as opposed to two spikes in control conditions (Figure 8D, right). The effects of NBQX were reversed upon washout (Figure 8D, bottom). 150 nM NBQX altered the complex spike in all of the four cells studied. These results further support the hypothesis that without saturation the climbing fiber would be sufficiently attenuated during physiological patterns of activity to affect its ability to produce a robust complex spike, which could influence the ability of the climbing fiber to induce long-term changes in synaptic strength.

Discussion

We found that a number of factors combine to make the climbing fiber synapse both powerful and reliable. Together, saturation of presynaptic calcium entry, of neurotransmitter release, and of postsynaptic receptors makes the EPSC insensitive to changes in calcium influx and near maximal in standard conditions. Although paired-pulse depression occurs, two properties of transmission combine to accelerate recovery of the postsynaptic response: residual calcium speeds the recovery of transmitter release and postsynaptic receptor saturation accentuates this rapid phase of recovery. In this way, even when climbing fibers are activated at high frequency, receptor saturation enables them to reliably drive Purkinje cells.

Mechanisms Contributing to EPSC Saturation

The climbing fiber to Purkinje cell synapse is typical of high p synapses in that the EPSC begins to saturate when Ca_e is increased. Saturation of presynaptic calcium entry contributed significantly to this EPSC saturation. In 2 Ca_e, calcium influx is half of that expected if there were a linear relationship between Ca_e and calcium influx (Figure 2). This reduction in calcium entry leads to a decrease in the EPSC amplitude that is shaped by the nonlinear relationship between EPSC amplitude and calcium entry (Figures 3A and 3B). The relationship between calcium influx and EPSC amplitude in the absence of AMPA receptor saturation (Figure 3C, DGG curve) allows us to estimate the effect of calcium influx saturation on neurotransmitter release. In 2 Ca_e, release is decreased by a factor of 4. Thus, saturation of presynaptic calcium entry is an important factor in limiting neurotransmitter release and ultimately in determining the extent of EPSC saturation.

By measuring presynaptic calcium influx, we took into account the saturation of calcium entry, which allowed us to examine additional mechanisms involved in EPSC saturation. Comparing the relationships between EPSC amplitude and Ca_{influx} in control conditions and in the presence of DGG revealed that AMPA receptor saturation makes an important contribution. Based on the relative block of DGG in different external calcium conditions (Figure 3C), AMPA receptor saturation does not attenuate the EPSC in low Ca_e but results in 4-fold and 7-fold reductions in EPSC amplitude in 2 Ca_e and 4 Ca_e, respectively (Figure 3D). The increasing prominence of AMPA receptor saturation is consistent with more prevalent multivesicular release in high Ca_e (Wadiche and Jahr, 2001).

An additional mechanism, most likely saturation of neurotransmitter release, accounts for the saturation of EPSC amplitude observed in the presence of DGG (Figure 3C). We estimate that saturation of release results in 1.9-fold and 3.6-fold reductions in EPSC amplitude in 2 Ca_e and 4 Ca_e, respectively (Figure 3D). This indicates that although saturation of neurotransmitter release contributes to the saturation of EPSC amplitude, contrary to widely held views, it is not the primary underlying mechanism.

Thus, three mechanisms contribute to saturation at this synapse. Under conditions of low calcium entry, when pre- and postsynaptic saturation are not factors, saturation of calcium influx limits neurotransmitter release and reduces the EPSC amplitude. Under standard conditions, AMPA receptor saturation is prominent and limits the amplitude of the EPSC, even though calcium influx is more attenuated than in low Ca_e. Although saturation of neurotransmitter release occurs, it is obscured by AMPA receptor saturation. The relative importance of

saturation of neurotransmitter release and postsynaptic receptor saturation are consistent with the number of docked vesicles present at individual release sites, multivesicular release, and postsynaptic receptor saturation. Because there are an average of seven docked vesicles at each release site (Xu-Friedman et al., 2001), multivesicular release leads to AMPA receptor saturation before there is significant saturation of release.

Factors Contributing to the Magnitude of Paired-Pulse Plasticity

We investigated both the Ca_{res} dependence and the contribution of postsynaptic receptor saturation to the paired-pulse ratio at this synapse in different Ca_e. In low Ca_e, Ca_{res} played an important role in determining the magnitude of short-term plasticity, but postsynaptic receptor saturation did not. Manipulating presynaptic calcium levels with EGTA eliminated facilitation (Figure 6C). Calcium measurements revealed that EGTA reduced the time constant of Ca_{res} decay by 86% and reduced the amplitude of Ca_{res} by 33%. Although we cannot measure Ca_{local} directly, these measurements provide an upper estimate of the reduction in Ca_{local}. The much larger effect of EGTA on Ca_{res} than on Ca_{local} suggests that EGTA eliminated facilitation primarily by affecting Ca_{res}, as at the parallel fiber synapse (Atluri and Regehr, 1996). DGG did not affect facilitation, indicating that saturation of postsynaptic receptors did not occur for such low p conditions.

The mechanisms governing the magnitude of the paired-pulse ratio are very different for conditions where the probability of release is high. Presynaptic calcium manipulations with EGTA did not influence the magnitude of PPR for stimulus pulses separated by 10 ms. This indicates that Ca_{res} has very little effect on the magnitude of PPR for high p conditions. However, DGG reduces the PPR from 0.40 to 0.32 in 2 Ca_e and from 0.25 to 0.15 in 4 Ca_e. Thus, AMPA receptor saturation limits the extent of depression in high p conditions (Wadiche and Jahr, 2001).

Contribution of Presynaptic Calcium and Postsynaptic Receptor Saturation to Recovery from Depression

We found that recovery from depression in high p conditions is influenced by both presynaptic residual calcium and by receptor saturation. In high Ca_e, there is a rapid and a slow phase of recovery from depression. Previous studies showed that EGTA reduced the rapid component of recovery from depression (Dittman and Regehr, 1998; Wang and Kaczmarek, 1998), although the effects of EGTA on Ca_{res} were not measured. Here we find that EGTA has a greater effect on Ca_{res} than on Ca_{local}, supporting a role for Ca_{res} in rapid recovery from depression.

AMPA receptor saturation also influences the time course of recovery from depression. In DGG, when AMPA receptor saturation is relieved, the recovery curve faithfully tracks changes in neurotransmitter release. DGG slowed both the rapid and slow phases of recovery and reduced the contribution of the rapid phase. These effects are readily explained by the sublinear relationship between the amount of neurotransmitter released and the EPSC amplitude. Saturation alters the recovery curve by attenuating larger EPSCs to a greater extent than the small EPSCs recorded at short interpulse intervals. As a result, in control conditions, AMPA receptor saturation accelerates recovery and accentuates the rapid recovery phase.

We have restricted our studies to climbing fiber synapses from relatively young animals because it is difficult to voltage clamp climbing fiber responses in older animals. However, climbing fiber responses measured in adult cats during trains and for pairs of stimuli (Eccles et al., 1966b) show remarkably similar use-dependent plasticity to the responses we report here. It is likely, therefore, that the mechanisms underlying the plasticity in our experiments are also present in older animals.

Physiological Implications of Postsynaptic Receptor Saturation

The influence of receptor saturation on short-term synaptic plasticity has important physiological consequences. Receptor saturation reduces the amount of depression during repetitive activation and accelerates subsequent recovery from depression. The extent of this effect can be seen in Figure 7, which reveals that following a train the EPSC amplitude is still significantly depressed in the absence of receptor saturation at a time when recovery is nearly complete in control conditions. The importance of saturation in maintaining climbing fiber efficacy during physiological trains is revealed when the synaptic strength is reduced in current clamp (Figures 8C and 8D). Reducing the synaptic efficacy to mimic the depression that follows a realistic train in control conditions does not significantly alter the Purkinje cell response to climbing fiber stimulation. However, reducing the conductance to mimic depression in the absence of receptor saturation changes the complex spike and its effect on spontaneous Purkinje cell firing (Figure 8C). Additionally, reducing the climbing fiber efficacy during brief trains in current clamp to mimic the removal of receptor saturation changes the Purkinje cell response. A reduced climbing fiber synaptic conductance will likely decrease the resulting elevation in dendritic calcium that is involved in long-term changes in synaptic strength. Thus, by limiting depression of the EPSC, receptor saturation makes transmission at this high p synapse more reliable, even during periods of relatively high activity.

Experimental Procedures

Electrophysiology

Sagittal slices (300 μM thick) were cut from the cerebellar vermis of 10- to 14-day-old Sprague Dawley rats as described previously (Dittman and Regehr, 1996; Llano et al., 1991). The external solution consisted of (in mM) 125 NaCl, 2.5 KCl, 2 $CaCl_2$, 1 $MgCl_2$, 26 $NaHCO_3$, 1.25 NaH_2PO_4, and 25 glucose, bubbled with 95% O_2/5% CO_2. For room temperature experiments, slices were superfused at 1 ml/min with the external solution. For high-temperature experiments (35°C), slices were superfused at 4 ml/min using a Gilson Minipuls pump, and saline was run through an inline heater (SH-27b with TC-324B controller, Warner Instruments). 20 μM bicuculline was included in the external solution to block $GABA_A$-mediated synaptic currents.

Whole-cell voltage clamp recordings of Purkinje cells were obtained as described previously (Regehr and Mintz, 1994). Glass electrodes (1–1.8 MΩ) were filled with an internal solution consisting of (in mM) 35 CsF, 100 CsCl, 10 EGTA, 10 HEPES, 0.2 D600, adjusted to pH 7.2 with CsOH. D600 was included to block L-type voltage-

gated calcium channels. The access resistance and leak current (−20 to −200 pA holding at −40mV) were monitored continuously, and experiments were rejected if either of these parameters increased significantly during the recording. Climbing fibers were stimulated by placing a glass electrode filled with external saline in the granule cell layer. The interstimulus interval between pairs of pulses was 40 s. Stimulation of climbing fibers in the granule cell layer can also activate parallel fibers, which exhibit paired-pulse facilitation, especially in low external calcium. Contamination of climbing fiber EPSCs by parallel fiber EPSCs would result in an underestimation of depression or an overestimation of facilitation. To avoid parallel fiber contamination, we adjusted the stimulus strength to just above threshold and analyzed failures to insure that there was no underlying parallel fiber EPSC.

For most experiments, currents were recorded at −40mV to inactivate Na^+ channels. Climbing fiber EPSCs were blocked with 250 nM of the high-affinity AMPA receptor antagonist NBQX in control conditions to minimize series resistance errors (~10-fold reduction at 24°C). It has been shown previously that NBQX and CNQX do not affect paired-pulse plasticity at the climbing fiber synapse (Dittman and Regehr, 1998; Hashimoto and Kano, 1998). In experiments in which DGG was used, we were not able to block the EPSC in control conditions with NBQX. In these experiments, the membrane potential was held more positive (−30mV to −20mV) to reduce the size of the EPSC. The concentration of DGG necessary to eliminate saturation was determined from experiments in which we assessed the ratio of the amplitudes of two EPSCs evoked 10 ms apart (paired-pulse ratio, PPR). DGG decreased the ratio of the amplitudes of these EPSCs in a dose-dependent manner. In 4 Ca_e, PPR was 0.20 ± 0.03, 0.19 ± 0.05, 0.16 ± 0.03, 0.13 ± 0.03, and 0.14 ± 0.04 in 0, 0.5, 1, 2, 5, and 10 mM DGG, respectively ($n = 3$). These findings indicate that in our experimental conditions the effect of DGG on PPR was maximal at concentrations between 2 and 5 mM. Therefore, we used 5 mM DGG throughout the rest of the study.

Whole-cell current clamp recordings of Purkinje cells were obtined using 2.5–3.5 MΩ electrodes containing (in mM) 130 $KMeSO_3$, 10 NaCl, 2 $MgCl_2$, 0.16 $CaCl_2$, 0.5 EGTA, 10 HEPES, 4 Na-ATP, 0.4 Na-GTP, 14 Tris-creatine phosphate, adjusted to pH 7.3. Climbing fibers were stimulated as above. In some experiments, 100–200 pA of hyperpolarizing current was injected to silence the spontaneous firing of the Purkinje cell.

Inferior Olive Injections

Injections were performed as described previously (Kreitzer et al., 2000). Briefly, P9–P12 rats were placed in a stereotaxic device and anesthetized with a continuous flow of a 1%–2% isoflurane/oxygen mixture. The brain stem was exposed using a dorsal caudal approach. Texas red dextran (10,000 MW) and the calcium indicator fluo-4 dextran (10,000 MW) were each dissolved in water at a concentration of 20%. These solutions were then mixed in a 1:1 ratio. This mixture was injected into the inferior olive with a Hamilton syringe.

Detecting Presynaptic Calcium Currents

Sagittal slices were cut from the cerebellar vermis of rats 2–4 days after injection. Fibers were illuminated with a Xenon bulb. Because fluo-4 is virtually nonfluorescent in the absence of calcium, labeled climbing fibers were identified by visualizing Texas red with rhodamine optics. These fibers were stimulated by placing a glass electrode in the granule cell layer near the ascending axon. Fluo-4 fluorescence was measured from the climbing fiber arborization with a photodiode. The filter set for fluo-4 dextran was 470DF20 for excitation, 510DRLP dichroic, and OG530 for emission. The filter set for Texas red dextran was 570DF10 for excitation, 590DRLP dichroic, and OG610 for emission (Omega Optical, Brattleboro, VT).

Data Acquisition and Analysis

Current clamp recordings were performed with an AxoClamp 2B amplifier. Voltage clamp recordings were performed with an Axopatch 200A amplifier. Outputs from both amplifiers and the photodiode were digitized with a 16 bit D/A converter (Instrutech, Great Neck, NY), with Pulse control software (Herrington and Bookman, 1995). EPSCs were filtered at 1 kHz with a 4 pole Bessel filter. Current clamp recordings were filitered at 10 kHz. Photodiode currents were digitally filtered offline at 200 Hz with a 4 pole Bessel filter. Analysis was performed using Igor Pro software (Wavemetrics, Lake Oswego, OR).

Acknowledgments

We thank Michael Beierlein, Dawn Blitz, Stephan Brenowitz, Solange Brown, Adam Carter, Patrick Safo, and Matthew Xu-Friedman for their comments on the manuscript. This work was supported by NIH R01-NS32405-01 and MH/NS32405-01 to W.G.R. and by a Howard Hughes Medical Institute Predoctoral Fellowship to K.A.F.

Received: June 3, 2002
Revised: October 23, 2002

References

Abbott, L.F., Sen, K., Varela, J.A., and Nelson, S.B. (1997). Synaptic depression and cortical gain control. Science *275*, 220–222.

Adler, E.M., Augustine, G.J., Duffy, S.N., and Charlton, M.P. (1991). Alien intracellular calcium chelators attenuate neurotransmitter release at the squid giant synapse. J. Neurosci. *11*, 1496–1507.

Armstrong, D.M., and Rawson, J.A. (1979). Activity patterns of cerebellar cortical neurones and climbing fibre afferents in the awake cat. J. Physiol. *289*, 425–448.

Atluri, P.P., and Regehr, W.G. (1996). Determinants of the time course of facilitation at the granule cell to Purkinje cell synapse. J. Neurosci. *16*, 5661–5671.

Betz, W.J. (1970). Depression of transmitter release at the neuromuscular junction of the frog. J. Physiol. *206*, 629–644.

Borst, J.G.G., and Sakmann, B. (1996). Calcium influx and transmitter release in a fast CNS synapse. Nature *383*, 431–434.

Brenowitz, S., and Trussell, L.O. (2001). Maturation of synaptic transmission at end-bulb synapses of the cochlear nucleus. J. Neurosci. *21*, 9487–9498.

Chen, C., and Regehr, W.G. (1999). Contributions of residual calcium to fast synaptic transmission. J. Neurosci. *19*, 6257–6266.

Chung, S., Li, X., and Nelson, S.B. (2002). Short-term depression at thalamocortical synapses contributes to rapid adaptation of cortical sensory responses in vivo. Neuron *34*, 437–446.

Clements, J.D., Lester, R.A., Tong, G., Jahr, C.E., and Westbrook, G.L. (1992). The time course of glutamate in the synaptic cleft. Science *258*, 1498–1501.

Diamond, J.S., and Jahr, C.E. (1997). Transporters buffer synaptically released glutamate on a submillisecond time scale. J. Neurosci. *17*, 4672–4687.

Dittman, J.S., and Regehr, W.G. (1996). Contributions of calcium-dependent and calcium-independent mechanisms to presynaptic inhibition at a cerebellar synapse. J. Neurosci. *16*, 1623–1633.

Dittman, J.S., and Regehr, W.G. (1998). Calcium dependence and recovery kinetics of presynaptic depression at the climbing fiber to Purkinje cell synapse. J. Neurosci. *18*, 6147–6162.

Dodge, F.A., and Rahamimoff, R. (1967). Co-operative action of calcium ions in transmitter release at the neuromuscular junction. J. Physiol. *193*, 419–432.

Eccles, J.C., Katz, B., and Kuffler, S.W. (1941). Nature of the "end-plate potential" in curarized muscle. J. Physiol. *124*, 574–585.

Eccles, J.C., Llinas, R., and Sasaki, K. (1966a). The excitatory synaptic action of climbing fibers on the Purkinje cells of the cerebellum. J. Physiol. *182*, 268–296.

Eccles, J.C., Llinas, R., Sasaki, K., and Voorhoeve, P.E. (1966b). Interaction experiments on the responses evoked in Purkinje cells by climbing fibres. J. Physiol. *182*, 297–315.

Feng, T.P. (1941). Studies on the neuromuscular junction. Chin. J. Physiol. *16*, 341–372.

Fogelson, A.L., and Zucker, R.S. (1985). Presynaptic calcium diffusion from various arrays of single channels. Implications for transmitter release and synaptic facilitation. Biophys. J. *48*, 1003–1017.

Granit, R., and Phillips, C.G. (1956). Spontaneous activity of cerebellar Purkinje cells and their responses to impulses in climbing fibers. J. Physiol. *133*, 520–547.

Hashimoto, K., and Kano, M. (1998). Presynaptic origin of paired-pulse depression at climbing fiber-Purkinje cell synapses in the rat cerebellum. J. Physiol. *506*, 391–405.

Heidelberger, R., Heinemann, C., Neher, E., and Matthews, G. (1994). Calcium dependence of the rate of exocytosis in a synaptic terminal. Nature *371*, 513–515.

Herrington, J., and Bookman, R.J. (1995). Pulse Control V4.5: IGOR XOPs for Patch Clmap Data Acquisition (Miami, FL: University of Miami).

Ito, M. (1984). The Cerebellum and Neural Control (New York: Raven Press).

Jenkinson, D.H. (1957). The nature of the antagonism between calcium and magnesium ions at the neuromuscular junction. J. Physiol. *138*, 434–444.

Katz, B., and Miledi, R. (1968). The role of calcium in neuromuscular facilitation. J. Physiol. *195*, 481–492.

Kreitzer, A.C., Gee, K.R., Archer, E.A., and Regehr, W.G. (2000). Monitoring presynaptic calcium dynamics in projection fibers by in vivo loading of a novel calcium indicator. Neuron *27*, 25–32.

Kusano, K., and Landau, E.M. (1975). Depression and recovery of transmission at the squid giant synapse. J. Physiol. *245*, 13–32.

Liley, A.W., and North, K.A.K. (1953). An electrical investigation of effects of repetitive stimulation on mammalian neuromuscular junction. J. Neurophysiol. *16*, 509–527.

Liu, G., Choi, S., and Tsien, R.W. (1999). Variability of neurotransmitter concentration and nonsaturation of postsynaptic AMPA receptors at synapses in hippocampal cultures and slices. Neuron *22*, 395–409.

Llano, I., Marty, A., Armstrong, C.M., and Konnerth, A. (1991). Synaptic- and agonist-induced excitatory currents of Purkinje cells in rat cerebellar slices. J. Physiol. *434*, 183–213.

Matthews, G. (1996). Neurotransmitter release. Annu. Rev. Neurosci. *19*, 219–233.

Mintz, I.M., Sabatini, B.L., and Regehr, W.G. (1995). Calcium control of transmitter release at a cerebellar synapse. Neuron *15*, 675–688.

Naraghi, M. (1997). T-jump study of calcium binding kinetics of calcium chelators. Cell Calcium *22*, 255–268.

Neher, E., and Augustine, G.J. (1992). Calcium gradients and buffers in bovine chromaffin cells. J. Physiol. *450*, 273–301.

Ramon y Cajal, S. (1911). Histologie du systeme nerveux de l'homme et des vertebres., Tome II edn (Paris, Maloine).

Regehr, W.G., and Mintz, I.M. (1994). Participation of multiple calcium channel types in transmission at single climbing fiber to Purkinje cell synapses. Neuron *12*, 605–613.

Roberts, W.M., Jacobs, R.A., and Hudspeth, A.J. (1990). Colocalization of ion channels involved in frequency selectivity and synaptic transmission at presynaptic active zones of hair cells. J. Neurosci. *10*, 3664–3684.

Schneggenburger, R., Meyer, A.C., and Neher, E. (1999). Released fraction and total size of a pool of immediately available transmitter quanta at a calyx synapse. Neuron *23*, 399–409.

Schwarz, C., and Welsh, J.P. (2001). Dynamic modulation of mossy fiber system throughput by inferior olive synchrony: a multielectrode study of cerebellar cortex activated by motor cortex. J. Neurophysiol. *86*, 2489–2504.

Silver, R.A., Momiyama, A., and Cull-Candy, S.G. (1998). Locus of frequency-dependent depression identified with multiple-probability fluctuation analysis in rat climbing fibre-Purkinje cell synapses. J. Physiol. *510*, 881–902.

Simon, S.M., and Llinas, R.R. (1985). Compartmentalization of the submembrane calcium activity during calcium influx and its significance in transmitter release. Biophys. J. *48*, 485–498.

Smith, P.D., Liesegang, G.W., Berger, R.L., Czerlinski, G., and Podolsky, R.J. (1984). A stopped-flow investigation of calcium ion binding by ethylene glycol bis(beta-aminoethyl ether)-N,N′-tetraacetic acid. Anal. Biochem. *143*, 188–195.

Stevens, C.F., and Wesseling, J.F. (1998). Activity-dependent modulation of the rate at which synaptic vesicles become available to undergo exocytosis. Neuron *21*, 415–424.

Tank, D.W., Regehr, W.G., and Delaney, K.R. (1995). A quantitative analysis of presynaptic calcium dynamics that contribute to short-term enhancement. J. Neurosci. *15*, 7940–7952.

Taschenberger, H., and von Gersdorff, H. (2000). Fine-tuning an auditory synapse for speed and fidelity: developmental changes in presynaptic waveform, EPSC kinetics, and synaptic plasticity. J. Neurosci. *20*, 9162–9173.

Tsodyks, M.V., and Markram, H. (1997). The neural code between neocortical pyramidal neurons depends on neurotransmitter release probability. Proc. Natl. Acad. Sci. USA *94*, 719–723.

Wadiche, J.I., and Jahr, C.E. (2001). Multivesicular release at climbing fiber-Purkinje cell synapses. Neuron *32*, 301–313.

Wang, L.-Y., and Kaczmarek, L.K. (1998). High-frequency firing helps replenish the readily releasable pool of synaptic vesicles. Nature *394*, 384–388.

Watkins, J.C., Pook, P.C., Sunter, D.C., Davies, J., and Honore, T. (1990). Experiments with kainate and quisqualate agonists and antagonists in relation to the sub-classification of 'non-NMDA' receptors. Adv. Exp. Med. Biol. *268*, 49–55.

Xu-Friedman, M.A., Harris, K.M., and Regehr, W.G. (2001). Three-dimensional comparison of ultrastructural characteristics at depressing and facilitating synapses onto cerebellar Purkinje cells. J. Neurosci. *21*, 6666–6672.

Zucker, R.S., and Regehr, W.G. (2002). Short-term synaptic plasticity. Annu. Rev. Physiol. *64*, 355–405.